UDC 548.736.442.6:539.261:548.4:001.57

Modelling of X-ray Diffraction Patterns from Nanostructured Perovskites $Sr(Fe,Co)O_{3-\delta}$

U. V. ANCHAROVA[1], S. V. CHEREPANOVA[2] and N. Z. LYAKHOV[1]

[1]*Institute of Solid State Chemistry and Mechanochemistry, Siberian Branch of the Russian Academy of Sciences, Ul. Kutateladze 18, Novosibirsk 630128 (Russia)*

E-mail: ancharova@gmail.com

[2]*Boreskov Institute of Catalysis, Siberian Branch of the Russian Academy of Sciences, Pr. Akademika Lavrentyeva 5, Novosibirsk 630090 (Russia)*

(Received December 7, 2011)

Abstract

Different models of defect ordering in strongly nonstoichiometric perovskite-like oxides based on strontium ferrites/cobaltites $Sr(Co_{0.8}Fe_{0.2})O_{3-\delta}$, $(Sr_{0.7}La_{0.3})(Co_{0.5}Al_{0.3}Fe_{0.2})O_{3-\delta}$, $(Sr_{0.7}Ca_{0.3})(Co_{0.5}Al_{0.3}Fe_{0.2})O_{3-\delta}$, $Sr(Co_{0.75}Nb_{0.05}Fe_{0.2})O_{3-\delta}$, $Sr(Co_{0.7}Nb_{0.1}Fe_{0.2})O_{3-\delta}$ and $Sr(Fe_{0.95}Mo_{0.05})O_{3-\delta}$ ($2.5 < (3-\delta) < 2.7$) are considered. Diffraction patterns of a number of samples differing in cation composition and degree of nonstoichiometry exhibit intensive reflections that are characteristic of the perovskite structural type with weak wider superstructural peaks. It is demonstrated by means of computer modelling of X-ray scattering on the crystals with different defects that such a diffraction pattern can correspond to three models of ordering of the oxygen vacancies: the formation of a homogeneous structure with the ordered state of oxygen vacancies (structural elements of the low-symmetry phase) and the formation of nano-heterogeneous systems (brownmillerite $ABO_{2.5}$ + perovskite ABO_3) of two types. In the first case, the components of the system have lamellar shape and interchange in one direction (a unidimensional disorder). In the second case we speak of the structure of brownmillerite domains turned with respect to each other at an angle of 90°, with different methods of redistribution of the perovskite component – at interfaces or in the form of separate domains. It is demonstrated with the help of two-dimensional diffraction of X-rays that this texture is observed not only at the nano-level but also for the samples with microdomains.

Key words: nanostructuring, perovskite, defects in crystals, synchrotron radiation, diffraction simulation

INTRODUCTION

Perovskite-like systems ABO_3 attract the attention of researchers due to a set of chemical and physical properties including ferroelasticity, mixed oxygen-ion conductivity *etc*. One of the most important factors determining the functional properties of simple $ABO_{3-\delta}$ and complex $AA'BB'O_{3-\delta}$ nonstoichiometric perovskites is their microdomain structure.

The presence of defects in real crystals is due to the fact that the accumulation of defects up to a definite concentration causes a decrease in the free energy of the system: $\Delta G = \Delta H - T\Delta S$. The formation of equilibrium defects is a thermodynamically allowed process because the formation of the majority of defects, though unfavourable from the viewpoint of energy, is favourable because of the increase of entropy. In this connection, real crystals always contain various kinds of defects distorting the ideal order [1, 2].

Strongly nonstoichiometric compounds have homogeneity regions in which the concentration of vacancies is achieved at a level providing their interaction between each other. Under definite conditions vacancies can form clusters or get redistributed over the lattice points

with the formation of ordered structures of different types including those with ordering of the clusters themselves [3]. At a temperature up to 700–1000 °C, thermodynamically equilibrium state of non-stoichiometric compounds is the ordered state, while the non-ordered state is metastable. So, nonstoichiometric solid solutions possess heterogeneous structure at the micro level. The widespread kinds of the assimilation of vacancies in the structure include the formation of the plane of crystallographic shear [2] or the structures of coherent joining [4], for example the series of $A_nB_nO_{3n-1}$ ($n \geq 2$) where, depending on the thickness of the block of octahedrons, brownmillerite or Grenier *etc*. phases arise.

Nonstoichiometric strontium ferrites/cobaltites $Sr(Fe,Co)O_{3-\delta}$ possessing mixed oxygen-electron conductivity are considered to be promising materials for the development of oxygen-permeable membranes and electrodes for solid oxide fuel elements [5]. Microheterogeneity can play a decisive role for these compounds because increased concentration of mobile defects on interfaces simplifies diffusion along the boundaries [6]. So, nanostructuring leads to the high concentration of channels for simplified diffusion of oxygen.

From the viewpoint of structure investigation, especially interesting are the samples with oxygen composition $2.5 < (3 - \delta) < 2.7$, that is, strongly nonstoichiometric perovskites with high defect content.

The goal of the present work is to reveal the methods of ordering extremely high defect concentration in the structure of strongly nonstoichiometric strontium ferrites/cobaltites.

Modelling of X-ray diffraction patterns of perovskite-like oxides based on $LaFeO_{3-\delta}$ was carried out in [7, 8], the methodological approach to the simulation of diffraction patterns on low-ordered systems was described by the authors of [9–12]. Previously we presented [13] the results of structural studies of nonstoichiometric $Sr(Fe,Co)O_{3-\delta}$, doped with non-isovalent cations with different degrees of oxygen nonstoichiometry, by means of the diffraction of synchrotron radiation. Modelling of X-ray diffraction patterns of nanostructured perovskites $Sr(Fe,Co)O_{3-\delta}$ with oxygen stoichiometry close to brownmillerite $2.5 \sim (3 - \delta) < 2.7$ was carried out for the first time. Structural studies of strongly nonstoichiometric strontium ferrites/cobaltites using a combination of experimental methods and computer simulation are necessary to confirm nanostructuring and approach the understanding of the kinetics of oxygen transport in these systems.

EXPERIMENTAL

Compounds under investigation ($Sr_{1-y}(La,Ca)_yCo_{0.8-z}(Al,Nb)_zFe_{0.2}O_{3-\delta}$ and $SrFe_{1-z}Mo_zO_{3-\delta}$, $0 \leq \delta \leq 0.5$) were synthesized using the standard ceramic method. Different kinds of treatment were used to change the oxygen stoichiometry of the samples: 1) slow cooling in a furnace; 2) subsequent annealing of the samples at 900 °C in the dynamic vacuum ($P \sim 10^3$ Pa) followed by quenching of the samples to room temperature; 3) annealing at 500 °C in the atmosphere of 5 % H_2/Ar followed by slow cooling in this atmosphere. Oxygen content in the samples was monitored by means of iodometric titration (the accuracy of determination was ±0.5 %) and agrees with the results of thermogravimetric method.

The synchrotron radiation (SR) of VEPP-3* storage was used for diffraction studies. Experiments were carried out at two experimental stations: 1) diffractometry with high resolution and anomalous scattering at the second channel of SR, VEPP-3 [14]; 2) diffractometry in high-energy X-rays 33.7 keV at the fourth channel of SR, VEPP-3 [15, 16].

Experiments at the second channel were carried out at the wavelength of 1.77 Å, $\Delta E/E \sim 10^{-4}$. The diffraction patterns from powder samples allowed us to process weak superstructural reflections with good accuracy and to distinguish the reflections with close positions.

At the experimental station of the fourth channel [15, 16], diffracted radiation was recorded with the help of a two-coordinate detector MAR-345 of Marresearch Co. on the basis of Image Plate. The spatial resolution was 100×100 μm, exposure 5–10 min (depending on current strength in the storage ring, which

*The equipment of the Shared Instrument Centre in Novosibirsk was used.

TABLE 1

Structural parameters of nonstoichiometric perovskites with superstructural reflections (see Fig. 1)

Sample No.	Chemical composition	Treatment method	$2a_p$, Å
1	$SrFe_{0.95}Mo_{0.05}O_{2.66}$	Quenched in vacuum	7.843
2	$SrCo_{0.8}Fe_{0.2}O_{2.64}$	Slowly cooled	7.728
3	$Sr_{0.7}La_{0.3}Co_{0.5}Al_{0.3}Fe_{0.2}O_{2.54}$	Quenched in vacuum	7.794
4	$Sr_{0.7}La_{0.3}Co_{0.5}Al_{0.3}Fe_{0.2}O_{2.49}$	Annealed in the atmosphere of 5 % H_2/Ar	7.814
5	$SrCo_{0.75}Nb_{0.05}Fe_{0.2}O_{2.45}$	Quenched in vacuum	7.803
6	$SrCo_{0.7}Nb_{0.1}Fe_{0.2}O_{2.47}$	The same	7.818

varied within the range 100–50 mA). The synchrotron radiation beam had a wavelength of $\lambda = 0.369$ Å, $\Delta E/E \sim 3 \cdot 10^{-3}$, the cross dimensions 0.4×0.4 mm, with extremely small beam divergence: angular spread was $(3 \cdot 10^{-3})°$.

2D-diffraction patterns were processed with the help of Area Diffraction Machine software by integrating over all the angles to obtain an averaged diffraction pattern $I(2\theta)$ over the recorded spatial angles.

Indexing by means of selection of an isostructural compound and refinement of the unit cell parameters using the least squares were carried out using PowderCell software (BAM Berlin). Diffraction patterns for the models of unidimensionally (1D) disordered crystal were calculated using the programme [9, 10] written in the Laboratory of Structural Methods of Investigation at the Institute of Catalysis, SB RAS (Novosibirsk). Diffraction patterns for the models of nanodomains were calculated using Debye equation.

RESULTS AND DISCUSSION

In the diffraction experiments involving SR, for a number of samples with different cation compositions (Table 1) and oxygen stoichiometry $2.45 < (3 - \delta) < 2.66$, specific diffraction phenomena are observed: at the background of narrow reflections indexed in the cubic perovskite cell ($Pm3m$ (#221), the lattice parameter of unit cell $a_p \sim 3.9$ Å) broadened low-intensity additional peaks arise (Fig. 1).

Each diffraction pattern can be indexed in the double cubic cell with dimensions $a_p \times 2a_p \times a_p$ (de Wolf criterion $M_{39} = 22 > 10$). Electron diffraction also reveals (see Fig. 1, *b*) additional broad reflections corresponding to the double cubic cell.

Homogeneous ordering of oxygen vacancies can proceed with the formation of a series of stoichiometric phases (brownmillerite, Grenier *etc.*); there is a discrete set of possible stoichiometric phases of defect ordering and corresponding oxygen stoichiometry of perovskite $ABO_{3-\delta}$, where $2.5 \le (3 - \delta) \le 3$.

According to the data of transmission electron microscopy (TEM) of perovskites under

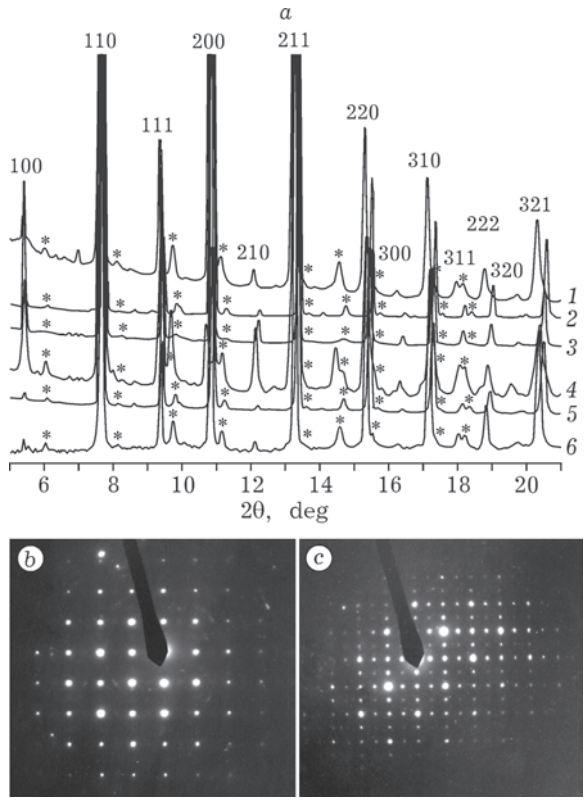

Fig. 1. Diffraction patterns of samples Nos. 1–6 (see Table 1) of nonstoichiometric perovskites with superstructural reflections (*), $\lambda = 0.369$ Å (*1–6*); *b*, *c* – electron diffraction on the samples with the composition $La_{0.3}Sr_{0.7}Co_{0.5}Fe_{0.2}Al_{0.3}O_{3-\delta}$ with different degree of oxygen nonstoichiometry: $3 - \delta = 2.68$ (*b*), 2.54 (*c*).

investigation, each element of the crystal with domain structure contains the phases characteristic of different types of vacancy ordering (mainly perovskite and brownmillerite structures; more rarely double perovskite, Grenier, Ruddlesden-Popper phases *etc.*). The diversity of stoichiometric phases and the presence of extended defects of the type of the planes of crystallographic shift or antiphase boundaries explain the fact that the values of oxygen stoichiometry for some samples (see Table 1) are smaller than those for an ideal brownmillerite structure $ABO_{2.5}$. According to the TEM data and experimental results from [17, 18], vacancy ordering is provided mainly by the coexistence of the domains with perovskite and brownmillerite structures. In this connection, considering the models of vacancy ordering in crystals, preferred are those in which the coherent joints of the blocks with exactly these compositions are assumed.

The nature of oxygen vacancy ordering was studied using computer modelling of diffraction patterns. We considered the possibilities of the homogeneous and nonhomogeneous ordering using various models.

Homogeneous ordering model

This model of the formation of superstructure implies vacancy ordering in the double cubic cell. We chose the cell $a_p \times 2a_p \times a_p$ composed of two perovskite cells; in each of them the coordinates of atoms corresponded to the symmetry group P*m*-3*m* (#221), $2a_p \sim 7.8$ Å.

A supercell with parameters $2a = b = 2c = 2a_p$ (Table 2) was found, so that the positions of all reflections corresponded with high accuracy to the diffraction pattern (Fig. 2, *a*) (rhombic symmetry group *Pmmm* (#47), de Wolf criterion $M_{22} = 38 > 10$). In this case the supercell is considered by us exclusively as an element of the heterogeneous system: the stoichiometric composition of this phase $ABO_{2.5}$ corresponds to brownmillerite but the oxygen composition of the compounds demonstrating superstructure in diffraction patterns varies within the range $2.45 < (3 - \delta) < 2.66$. According to TEM data [17, 18] and the results of Mossbauer spectroscopy, the prevalence of brownmillerite components of the heterogeneous system $ABO_3 + ABO_{2.5}$ is evident. In this connection, this model of vacancy ordering is improbable in our opinion in comparison with the nonhomogeneous ordering participated by the domains of brownmillerite structure.

TABLE 2

Atomic coordinates in the double cubic perovskite cell $a_p \times 2a_p \times a_p$. Symmetry group *Pmmm* (#47)

Atoms	Position	*x*	*y*	*z*
Sr	2*p*	0.50	0.25	0.50
Fe	1*a*	0	0	0
Fe	1*e*	0	0.50	0
O	1*b*	0.50	0	0
O	1*c*	0	0	0.5
O	2*m*	0	0.25	0
O	1*f*	0.50	0.50	0
O*	1*g*	0	0.50	0.50

* Coordinates of oxygen vacancies.

Inhomogeneous ordering model

Along one direction in the crystal. According to the TEM data, this model assumes alternation of coherently joined lamellar components with perovskite and brownmillerite structures. Perovskite structure can be represented as a sequence of the layers of octahedrons (O), while brownmillerite structure is an alternation of the layers of octahedrons and tetrahedrons (OTOT′). In the general case, distortion of the order in one direction causes the appearance of diffuse scattering. Modelling the diffraction patterns we showed that diffuse scattering is concentrated exactly in the region of superstructural peaks (see Fig. 2, *b*). For modelling phase joint, we used the spatially rotated (built on the diagonals) cell of perovskite structure ($a = a_p 2^{1/2}$; $b = a_p$; $c = a_p 2^{1/2}$) and the cell of brownmillerite structure deformed along *a* and *c* axes ($a = a_p 2^{1/2}$; $b = b_b$; $c = a_p 2^{1/2}$). Taking into account the oxygen stoichiometry $ABO_{2.6}$, the ratio of phases with perovskite and brownmillerite structures should be equal to 4 : 1. So, the average thickness of the sheet with brownmillerite structure should be four times larger than the average thickness of the sheet

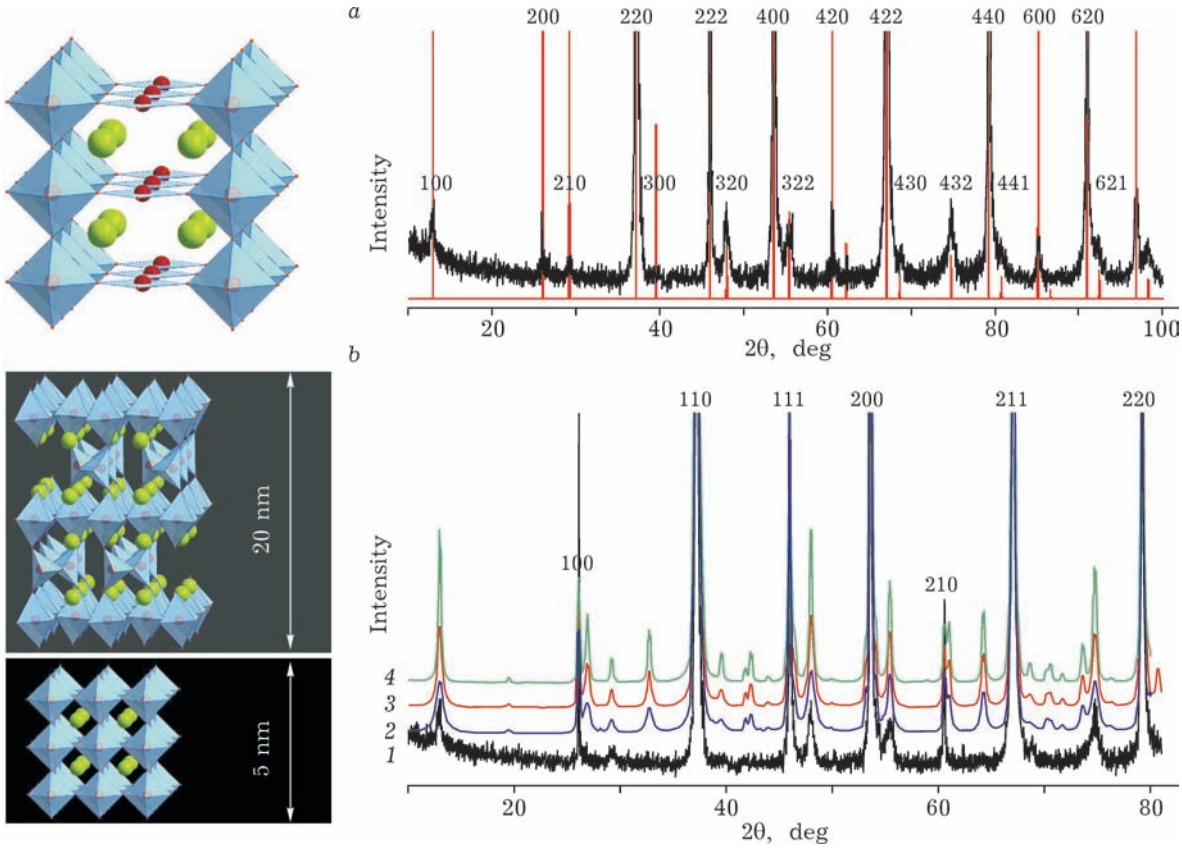

Fig. 2. Model of homogeneous ordering of vacancies (*a*) and nonhomogeneous ordering of perovskite and brownmillerite structures $ABO_3 + ABO_{2.5}$ along one direction of the crystal (*b*): *1* – experimental diffraction pattern of sample $SrFe_{0.95}Mo_{0.05}O_{2.66}$ quenched in vacuum; *2–4* – probability of grouping of ($ABO_{2.5}$) cells: P_{22} = 0.7 (*2*), 0.8 (*3*), 0.9 (*4*); λ = 1.77 Å; red lines (*a*) – calculated position of diffraction maxima.

with perovskite structure. Therefore, there should be one sheet of the OTOT′ type per one sheet of O type because the former sheet is about 4 times thicker than the latter one. Having determined the probability of the appearance of OTOT′ layer as W_2 = 0.5, we assign the stoichiometrically necessary ratio of the thicknesses of layered components. The absolute values of layer thickness are determined by the probability parameter of brownmillerite-like layers grouping P_{22} (the relative probability of the OTOT′ type layer following the OTOT′). The larger is P_{22}, the larger is the thickness of the sheets with brownmillerite and perovskite structures.

The calculated diffraction patterns provide a good description of the positions of both major and additional peaks. The average coherent length (for model particles) calculated from the width of narrow major peaks is approximately equal to 75 nm. The thickness of the sheets (P_{22} was the variable parameter) affects the intensity of additional peaks. Experimental and calculated data agree with each other to the maximal extent in the case of the model for which the average thickness of the sheets with perovskite and brownmillerite structures is 5 and 20 nm, respectively. This model suggests that the present diffraction reflections can be connected with nanostructuring according to the type of coherent joining of two ordered phases. Moreover, vacancy-ordered ideal $ABO_{3-\delta}$ structure should have the following composition with respect to oxygen: $(3 - \delta)$ = 2.5 (OTOT′), 2.67 (OOT), 2.75(OP, OOOT), 2.8 (OOOOT), 2.83 (OOP, OOOOOT); ... 3(O), where O – octahedrons, T – tetrahedrons, P – pentahedrons. One can see that oxygen-deficient compositions ~$ABO_{2.6}$ do not get into any stoichiometric phase, which points to the heterogeneous state of the structure built by the two types of the domains of stoichiometric phases.

So, the structure of these nonstoichiometric perovskite-like materials can be represented as brownmillerite system alternating with perovskite fragments in which the whole amount of oxygen above the stoichiometric value is accumulated ($0.5 - \delta$), and maybe polyvalent cations too.

Over the whole crystal volume (nanodomain system). The model was chosen in which deformed brownmillerite $a_{b/m} = c_{b/m} = 2^{2/1}a_p$; $b_{b/m} = 4a_p$) blocks with dimensions $8 \times 16 \times 8$ and $5 \times 5 \times 5$ mm (Fig. 3, *a* and *b*, respectively) have three equivalent mutually perpendicular orientations, are coherently jointed with each other; taking into account oxygen stoichiometry, they alternate with perovskite blocks of the corresponding size. For modelling, we used the programmes for the calculation of diffraction patterns from a structured particle according to Debye's equation. Several versions of block joints were considered. In one version, particle size is $40 \times 40 \times 40a_p^3$ (~15.5 nm in section), the size of brownmillerite blocks is $40 \times 20 \times 20a_p^3$, perovskite $20 \times 20 \times 20a_p^3$, the blocks are in junction with each other without sublayers (twins) (see Fig. 3, *a*). Another version implies the presence of a particle with a size $39 \times 39 \times 39a_p^3$ (~15 nm in section, see Fig. 3, *b*) composed of 27 brownmillerite domains ($12 \times 12 \times 12a_p^3$) of three different orientations, alternating with perovskite sublayers, with thickness a_p.

The diffraction patterns exhibit a specific type of diffraction phenomena: the high symmetry of the perovskite matrix is partially conserved in such a manner that the superposition of nanodomains leads to the appearance of diffraction patterns with apparent cubic perovskite structure and additional superstructural reflections. Inside the domains, local order in the nearest neighbourhood is observed, while point defects – the atoms of over-stoichiometric oxygen x ($ABO_{2.5+x}$) are displaced to domain boundaries.

So, the whole excess oxygen is displaced to domain walls. The relative density of domain walls within the crystal volume is given by the

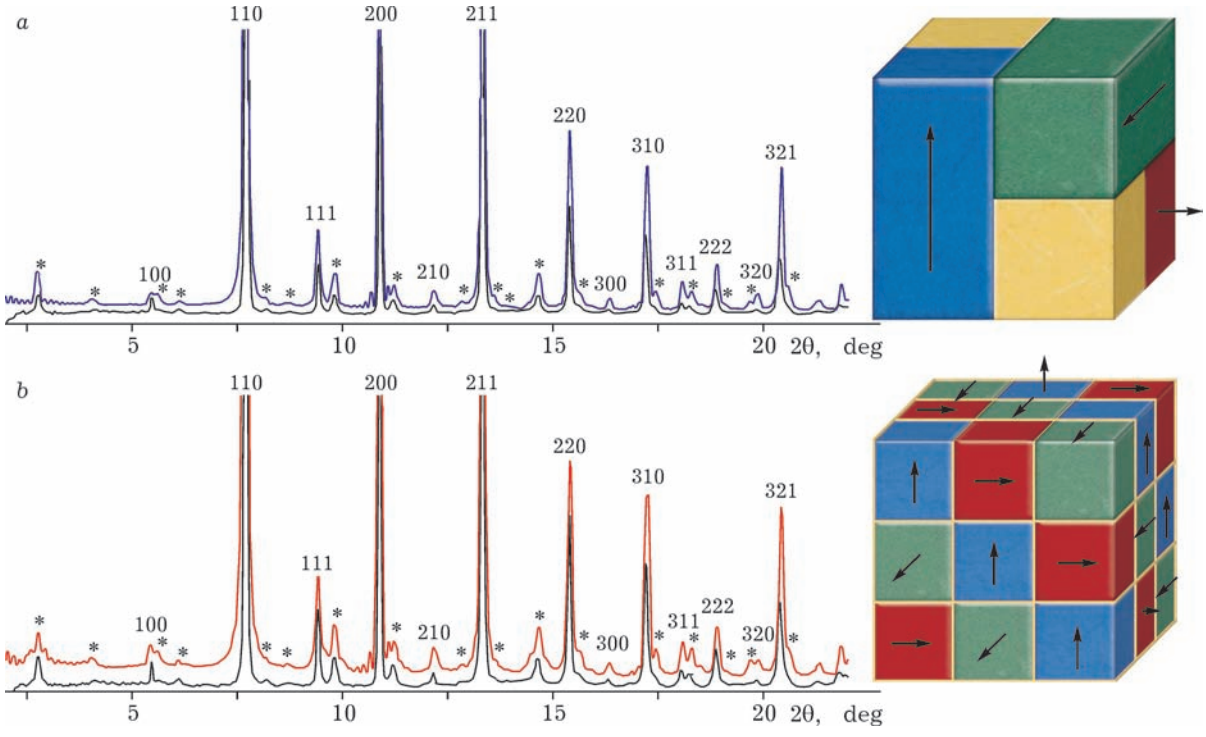

Fig. 3. Modelling of the nanodomain system and calculation of diffraction patterns using Debye formula for the composition $SrFe_{0.95}Mo_{0.05}O_{2.66}$ (black lines – experimental diffraction patterns, red and blue lines – calculated ones; yellow regions – perovskite structure, red, blue and green regions – brownmillerite structure): *a* – particle about 15.5 nm in size is composed of five blocks – three orthogonal brownmillerite and two perovskite; *b* – particle about 15 nm in size is composed of 27 brownmillerite blocks of three orthogonal types with perovskite sublayer between them, $\lambda = 0.369$ Å; arrows indicate the directions of the *b* axis of the structure of domains of the low-symmetry phase.

value of superstoichiometry with respect to oxygen ($x = 0.5 - \delta$) and depends on the size of domains with brownmillerite structure because it is proportional to the total area of domain surface in the crystal. One can see in the data of Fig. 1 that the diffraction patterns of the samples identical in cation composition but differing from each other in the degree of oxygen nonstoichiometry (curves *3*, *4*) differ in the intensity of additional diffraction maxima: with a decrease in superstoichiometry ($0.5 - \delta$) the intensity of additional reflections increases. Calculating scattering intensity according to Debye formula for the particles of the same diameter but with different domain sizes, it was discovered that additional reflections become more intense with an increase in domain size, while the width of reflections does not change. Therefore, the differences in the intensity of additional maxima for curves *3* and *4* (see Fig. 1) depict the differences not only in oxygen stoichiometry but also in the size of domains in crystals.

The appearance of coupled rings on the 2D diffraction picture from brownmillerite ($Sr_{0.7}Ca_{0.3}Co_{0.5}Al_{0.3}Fe_{0.2}O_{2.5}$ and $Sr_{0.5}Ca_{0.5}Co_{0.5}Al_{0.3}Fe_{0.2}O_{2.5}$) samples points in favour of the microtwinning model: the distribution of spots (texture) from separate crystallites over the perimeter of one ring is repeated at the neighbouring one [13]. This effect is observed only for reflections that belonged to the cubic system before the symmetry was reduced, and then underwent the rhombic splitting (Fig. 4). In the general case, texture maxima from different planes ((*hkl*), (*lkh*), (*khl*) *etc.*) should lie on the 2D picture in different azimuthal directions determined by the geometry of the lattice. As a consequence, the neighbouring coupled spots cannot belong to one crystallite, so the observed effect is due to the orientation of blocks with respect to each other.

According to Curie principle, in the case of distortions caused by temperature action, the formed domains orient in such a manner that the initial symmetry is conserved averaged over many domains. In the case under consideration, with symmetry reduction from cubic to rhombic when averaged over all domains, the axis of the 3rd order should be recovered [19]. To achieve this, twinning should proceed in three mutually perpendicular directions. As a result, the reciprocal space of the local variety of domains that underwent twinning will be a superposition of six reciprocal spaces of mutually perpendicular twins because the orientation of a block during phase transition arises along any of the initial directions (*a*, *b*, and *c*). In other words, a pair (or more) of blocks appears so that deforming in the perpendicular directions they inherited the initial cubic orientation. So, macroscopically (for a group of domains) those symmetry elements that disappeared during the phase transition into the low-

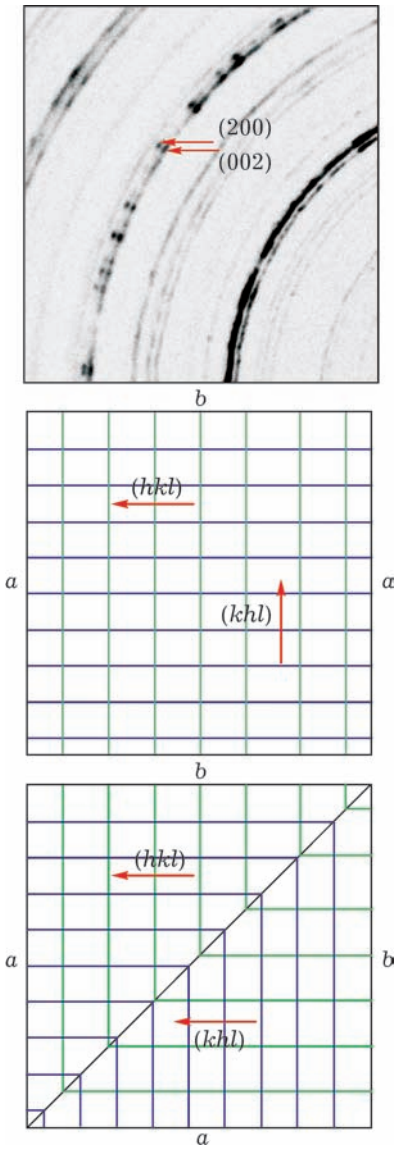

Fig. 4. Fragment of the 2D diffraction picture of brownmillerite composition $Sr_{0.7}Ca_{0.3}Co_{0.5}Fe_{0.2}Al_{0.3}O_{2.5}$, λ = 0.369 Å. The scheme of the appearance of double reflections as a result of twinning in the structure.

symmetry phase are recovered. Therefore, the maximum on one ring forms a pair with the maximum on another ring that arises from the neighbouring blocks oriented perpendicularly.

In the case of an ideal crystal, two diffraction maxima from one crystallite with different interplane spacings d_1 and d_2 can go into the reflecting position simultaneously only if the relative scattering of the spectral width of X-ray radiation $\Delta E/E$ over angles $\Delta 2\theta_S = 2\text{tg}\,\theta(\Delta E/E)$ exceeds the angular distance between reflections $\Delta 2\theta_R = 2(\arcsin(\lambda/2d_1) - \arcsin(\lambda/2d_2))$. In experiment (see Fig. 4) for double reflections $\Delta 2\theta_S \sim 0.06° < \Delta 2\theta_R \sim 0.2°$, therefore, the domain structure of the crystal is substantially non-ideal. The nonideality of the structure is manifested as the appearance of small-angle boundaries between microdomains due to the mismatch of atomic rows on domain boundaries. The degree of deviation from the ideal crystal state and the value of small-angle boundaries can be estimated from the azimuthal width of diffraction maxima on the 2D diffraction picture (see Fig. 4) $\Delta 2\theta_A \sim 4°$, which exceeds the values $\Delta 2\theta_S$ and $\Delta 2\theta_R$. So, inheriting the orientation of the highly symmetric phase, the blocks with brownmillerite structure created mosaic morphology of microdomains in the crystal, similar to the nanodomain state (see Fig. 3).

Depending on the size of twins, different diffraction effects are observed: at the nano level – the diffraction pattern with narrow intense perovskite reflections and broadened weak additional reflections; at the micro level – coupled texture maxima on diffraction rings are formed.

CONCLUSION

Strongly nonstoichiometric perovskite-like oxides based on strontium ferrite-cobaltite were studied by means of X-ray diffraction. For a number of samples with different cation composition and degree of nonstoichiometry $2.5 < (3 - \delta) < 2.7$, effects of nanostructuring are observed. They manifest themselves as weak broad additional peaks at the background of intense peaks characteristic of the structural type of perovskite. Using the computer modelling of diffraction on crystals with defects, we considered different models of ordering the oxygen vacancies: one-dimensional ordering as a separate phase in which oxygen vacancies are a structural element, and nonhomogeneous ordering as the coherent coexistence of the two extreme states of the solid solution ABO_3 + $ABO_{2.5}$ with perovskite and brownmillerite structures, respectively. For nonhomogeneous ordering, three types of structures were considered: one-dimensionally disordered components, twins and three-dimensionally ordered domains. It was shown that oxygen vacancies in strongly nonstoichiometric perovskite-like systems get ordered through the formation of the structure of brownmillerite nanodomains turned with respect to each other at an angle of 90° with the distribution of perovskite component at the boundaries between domains. It was shown that this texture is observed not only at the nanolevel but also in the case of the samples with microdomains.

REFERENCES

1 Ariya S. M., Popov V. G., *Zh. Obshchey Khim.*, 32(1962) 2077.
2 West A. R., Solid State Chemistry and Its Applications, Wiley, New York, 1987.
3 Anderson J. S., Problems of Nonstoichiometry, North-Holland, Amsterdam, 1970.
4 Hodges J. P., Short S., Jorgensen J. D., Xiong X., Dabrowski B., Mini S. M., Kimball C. W., *J. Solid State Chem.*, 151 (2000) 190.
5 Bouwmeester H. J. M., Burgraaf A. J., in: Fundamentals of Inorganic Membrane Science and Technology, in A. J. Burgraaf and L. Cot (Eds.), Elsevier, Amsterdam, 1996, 435.
6 Salje E. K. H., Hayward S. A., Lee W. T., *Foundations of Crystallography*, 61, 1 (2005) 3.
7 Cherepanova S. V., Tsybulya S. V., *Zeitschrift für Kristallographie*, 27, 1 (2008) 5.
8 Nadeev A. N., Tsybulya S. V., Gerasimov E. Yu., Kulikovskaya N. A., Isupova L. A., *Zh. Strukt. Khim.*, 51, 5 (2010) 927.
9 Cherepanova S. V., Tsybulya S. V., *J. Mol. Catal. A: Chem.*, 158, 1 (2000) 263.
10 Cherepanova S. V., Modelirovaniye Struktury Chastichno Razuporyadochennykh Ultradispersnykh Materialov na Osnove Polnlprofilnogo Analiza Poroshkovykh Difraktsionnykh Kartin (Candidate's Dissertation in Physics), Novosibirsk, 2000.
11 Proffen T., Neder R. B., *J. Appl. Cryst.*, 30 (1997) 171.
12 Neder R. B., Proffen T., Diffuse Scattering and Defect Structure Simulations, University press, Oxford, UK, 2008.
13 Ancharova U. V., Ancharov A. I., Lyakhov N. Z., Nemudry A. P., Pyatiletova E. V., Savinskaya O. A., Tsybulya S. V., J. *Nuclear Instr. and Methods in Physics Res. Section A: Accelerators, Spectrometers, Detectors and Associated Equipment*, 575 (2007) 144.

14 Shmakov A. N.
URL: http://ssrc.inp.nsk.su/CKP/stations/passport/2/
15 Ancharov A. I.,
URL: http://ssrc.inp.nsk.su/CKP/stations/passport/4/
16 Ancharov A. I., Manakov A. Yu., Mezentsev N. A., Tolochko B. P., Sheromov M. A., Tsukanov V. M., *J. Nuclear Instr. and Methods in Physics Res. Section A: Accelerators, Spectrometers, Detectors and Associated Equipment*, 470 (2001) 80.
17 Nakayama N., Takano M., Inamura S., Nakanishi N., Kosuge K., *J. Solid State Chem.*, 71, 2 (1987) 403.
18 Alario-Franco M. A., Gonzalez-Calbet J. M., Vallet-Regi M., Grenier J. S., *J. Solid St. Chem.*, 49, 2 (1983) 219.
19 Curie P., Simmetriya v Fizicheskikh Yavleniyakh (Izbrannye Trudy), Nauka, Moscow, 1966.